Theoretical surface-enhanced Raman spectra study of substituted benzenes II. Density functional theoretical SERS modelling of *o*-, *m*-, and *p*-methoxybenzonitrile

Guillermo Diaz Fleming [a,*], Italo Golsio [a], Andres Aracena [a], Freddy Celis [a], Leticia Vera [a], Rainer Koch [b], Marcelo Campos-Vallette [c]

[a] *Molecular and Atomic Spectroscopy Laboratory, Department of Chemistry, Faculty of Sciences University of Playa Ancha, Valparaiso, Casilla 34-V, Chile*
[b] *Institute for Pure and Applied Chemistry and Center of Interface Science, University of Oldenburg, P.O. Box 2503, D-26111 Oldenburg, Germany*
[c] *Molecular Spectroscopy Laboratory, Department of Chemistry, Faculty of Sciences, University of Chile, Casilla 653, Santiago, Chile*

A B S T R A C T

The SERS modelling of *o*-, *m*-, and *p*-methoxybenzonitrile has been performed following the same methodology that in Part I. Optimized structure obtained from DFT calculations in a B3LYP-LANL2DZ level of calculation shows different tilted positions for the isomers under study. From correlations obtained by comparison of Raman and SERS spectra concerning geometrical parameters, frequency shifting, change in band intensity, and force constants is possible to give insight about the different effect of the metal surface on these molecules and the structural reasons of this behaviour. Frontier orbital analysis gives further information and reveals a ligand to metal charge transfer mechanism for all isomers, as well as its relative importance.

Keywords:
DFT calculations
SERS spectra modelling
Methoxybenzonitrile

1. Introduction

On the base of DFT calculations in Part I [1] it was concluded that the mechanism affecting the SERS spectrum of benzonitrile (BN) is mainly charge transfer (CT) in nature. The aim of this paper is to examine how well the model and theoretical considerations previously reported to obtain reliable insight into the SERS mechanism for BN, will be able to lead to consistent results in the monosubstituted derivatives of this molecule. Furthermore, we want to inquire about changes eventually produced in the orientation of these molecules on a metallic surface as a consequence of the position of the pendant group in the BN ring, as well as to quantify the degree of the CT mechanism involved in each molecule. The methoxy group is suitable to study such a perturbation because of its strong donor character and its consequent electronic effect on the CN group.

Experimental vibrational studies, as well as normal coordinate analysis of *p*- and *m*-methoxybenzonitrile, have been performed by Kumar and Rao [2,3]. Electronic and vibrational spectra and thermodynamic functions of *m*- and *p*-methoxybenzonitrile have been reported by Goel and Agarwal [4].

SERS spectra of *o*-, *m*-, and *p*-methoxybenzonitrile have been studied by Boo et al. [5]. In that work has been reported qualitatively a tilted orientation of these molecules on the silver surface in the basis of the SERS selection rules [6] but they cannot arrive to definitive conclusions without new experiments, so that the present work can give more insight on the orientation and the SERS mechanism from a theoretical point of view.

In the SERS modelling of *o*-, *m*-, and *p*-methoxybenzonitrile we have considered the same methodology as in Part I, although the emphasis is focused on the comparison of the SERS effect in the different isomers, as well as on the structural reasons of this behaviour.

2. Computational methods

Calculations of the structure and vibrational spectra of the investigated compounds were performed using the Gaussian 03 program package [7]. All calculations were carried out with Becke's three-parameters hybrid method using the Lee–Yang–Parr correlation functional (B3LYP) [8,9] together with the LANL2DZ basis set corresponding to the D95 basis on first row atoms [10] and the Los Alamos DZ on silver [11]. For the optimized structure of the examined species no imaginary frequencies modes were obtained, proving that a local minimum on the potential energy surface was

* Corresponding author at: Molecular and Atomic Spectroscopy Laboratory, Department of Chemistry, Faculty of Sciences, University of Playa Ancha, Avenida Playa Ancha 350, Valparaiso, Casilla 34-V, Chile. Tel.: +56 32 2500528.
E-mail addresses: guillermodiaz@upla.cl, ruben_diaz@entelchile.net (G.D. Fleming).

Table 1
Calculated bond lengths (Å) of the three methoxybenzonitriles

	OMBN	MMBN	PMBN
C–C ring	1.407	1.411	1.413
C–H ring	1.087	1.085	1.086
C ring-O	1.385	1.392	1.388
C–CN	1.437	1.441	1.437
O–C methyl	1.460	1.458	1.460
C–N	1.183	1.183	1.184
C–H methyl	1.098	1.099	1.098

Table 2
Calculated and experimental thermodynamic functions (cal/mol K) for OMBN, MMBN, and PMBN at 298.15 K

		This work	Experimental [4]
OMBN	S^0	91.40	–
	C_p^0	34.33	–
MMBN	S^0	91.45	87.08
	C_p^0	34.34	32.50
PMBN	S^0	91.56	86.98
	C_p^0	34.32	32.45

Table 3
Calculated bond lengths (Å) of the three methoxybenzonitrile–silver complexes

	OMBN–Ag	MMBN–Ag	PMBN–Ag
C–C ring	1.423	1.409	1.415
C–O	1.383	1.391	1.386
C–CN	1.433	1.438	1.434
C–H ring	1.086	1.085	1.086
O–Me	1.461	1.459	1.461
C–H methyl	1.098	1.099	1.098
N–Ag	2.543	2.550	2.562
C–N	1.181	1.181	1.182

Table 4
Selected geometrical parameters values of the three methoxybenzonitriles and methoxybenzonitrile–silver complexes (SERS)

	CN (Å)	N–Ag (Å)	C–N–Ag (°)	Ring-O (Å)	O–Me (Å)	C–CN (Å)
OMBN	1.183			1.385	1.456	1.437
OMBN–Ag	1.181	2.543	152.7	1.383	1.461	1.433
MMBN	1.183			1.392	1.458	1.440
MMBN–Ag	1.181	2.550	152.7	1.391	1.460	1.438
PMBN	1.183			1.388	1.457	1.437
PMBN–Ag	1.182	2.562	148.8	1.386	1.461	1.434

Table 5
Selected diagonal stretching force constants (mdyn/(Å)

	OMBN	OMBN–Ag	MMBN	MMBN–Ag	PMBN	PMBn–Ag
Ring						
CC (M)	5.31	5.14	5.24	5.25	5.13	5.11
CC (M, CN)*	5.14	5.00	5.32	5.30	5.23	5.19
CC (CN)	5.02	5.17	5.08	5.07	5.06	5.01
CC	5.13	5.14	5.12	5.09	5.21	5.06
CH	5.66	5.70	5.65	5.66	5.72	5.72
Ring-CN						
C–CN	5.93	5.94	5.79	5.78	5.88	5.90
CN	17.56	17.53	17.58	17.53	17.45	17.37
Ring-M						
CO	6.00	6.04	5.86	5.89	5.94	5.98
Methoxy						
O–C	4.71	4.68	4.75	4.72	4.71	4.70
CH	5.27	5.28	5.25	5.26	5.27	5.28
CH	5.27	5.29	5.25	5.26	5.27	5.27
CH	5.57	5.58	5.56	5.56	5.55	5.57
N–Ag		0.19		0.15		0.16

(M) and/or (CN) indicates that the CC stretching is related to methoxy (M) and/or nitrile (CN) groups, *only OMBN.

found. The energies of the Frontier orbitals discussed in the last section are in fact those of the β orbitals, close examination showed that there is almost no difference to the corresponding α orbitals with the additional α spin orbital (a HOMO) being located purely on the Ag atom.

Calculated wavenumbers have been scaled by 0.9695 to account for anharmonic behavior incomplete incorporation of electron correlation and the use of finite basis sets in the theoretical treatment. This value has been applied to all regions of the spectra, so it is possible that some vibrations are affected stronger than others [12].

Conversion from Cartesian to internal coordinates and decomposition of the potential energy distribution (PED) was carried out using the program FCART01, a major modification of previous software [13]. With the internal force constants matrices of the PED are obtained which provide a measure of each internal coordinate's contribution to the normal coordinate at the above-mentioned theoretical level. For the sake of brevity, the complete tables of the

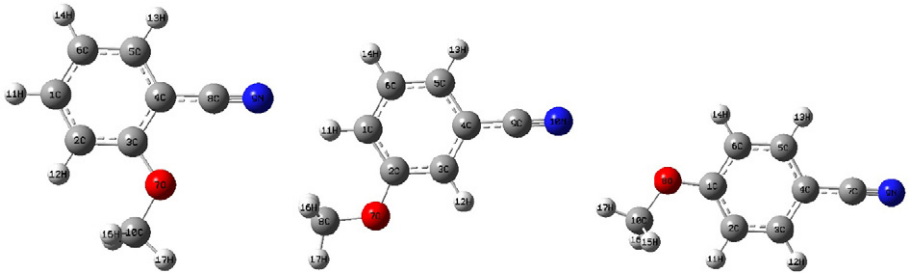

Fig. 1. B3LYP/LANL2DZ-optimized structures of *o*-methoxybenzonitrile (OMBN), *m*-methoxybenzonitrile (MMBN) and *p*-methoxybenzonitrile (PMBN).

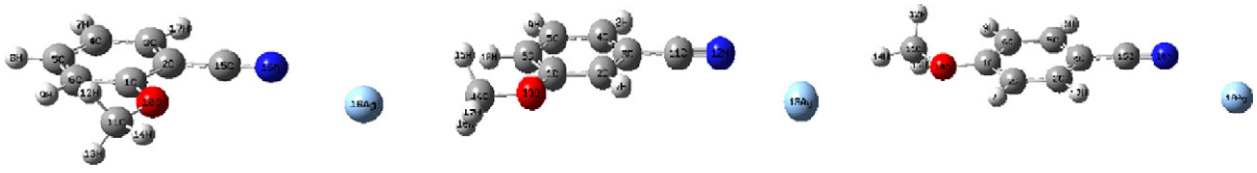

Fig. 2. B3LYP/LANL2DZ-optimized structures of the OMBN–Ag (left), MMBN–Ag (center) and PMBN–Ag complex (right).

Table 6
Calculated Raman frequencies (cm^{-1}) and intensities ($Å^4$/amu) of the methoxybenzonitriles

OMBN		MMBN		PMBN		Assignment
Frequency	Intensity	Frequency	Intensity	Frequency	Intensity	
122	1	134	5	126	0	CH_3–BN torsion
129	6	151	0	137	3	CCN–CH_3 in-plane bending
203	1	199	3	205	1	CH_3 torsion
238	0	243	2	238	2	BN–CH_3 in-plane bending
257	0	258	0	275	0	CH_3 torsion, BN out-of-plane bending
394	3	392	3	370	10	Ring in-plane, CCN bending in-plane
400	8	395	8	414	0	BN (meta) in-plane bending, CCN bending in-plane
437	6	455	3	471	4	Ring (CN) symm in-plane bending
497	2	479	2	478	2	Ring (meta) out-of-plane bending
566	7	528	7	550	3	Ring asymm in-plane bending
577	2	581	1	561	3	CCN in-plane bending
585	3	628	3	638	6	Ring (CN) symm out-of-plane bending, CCN out-of-plane bending
708	22	695	0	660	1	Ring (meta) symm in-plane bending
752	1	696	14	736	1	CH symm out-of-plane bending
771	0	805	0	791	40	CH asymm out-of-plane bending, BN asymm out-of-plane bending
791	3	858	5	831	0	Trigonal breathing, CO stretching, O–CH_3 stretching
873	0	904	1	854	0	CH asymm out-of-plane bending, ring symm out-of-plane bending
964	0	919	0	969	0	CH symm out-of-plane bending
983	4	976	41	982	2	Trigonal breathing, O–CH_3 bending
1000	0	993	1	986	0	CH asymm out-of-plane bending
1031	30	1013	9	998	0	CC asymm stretching (1)
1102	1	1086	3	1110	1	CC asymm stretching (2)
1117	8	1116	9	1115	8	CH_3 rocking *xz* plane
1153	4	1136	3	1156	8	CH_3 rocking *yz* plane
1174	8	1162	8	1176	51	CH (ortho) in-plane bending, ring in-plane deformation
1183	19	1184	7	1193	29	CH (para) in-plane bending out-of-plane
1240	30	1247	33	1238	12	CH in-plane bending C–O stretching
1278	2	1293	1	1306	2	Trigonal breathing
1329	10	1342	7	1325	7	CH in-plane bending CC stretching
1425	1	1423	2	1411	4	CH_3 bending symm
1445	4	1443	14	1438	7	CH_3 bending symm, CC stretching, CH in-plane bending
1467	5	1469	2	1469	25	CH_3 bending asymm, CC stretching, CH in-plane bending
1471	22	1471	24	1470	10	CH_3 bending asymm
1482	16	1472	10	1494	12	CH_3 out-of-phase deformation
1576	14	1571	22	1559	8	CC asymm stretching, CH_3 out-of-phase deformation
1594	80	1607	62	1610	174	CC symm stretching, CO stretching
2198	397	2197	435	2189	626	CN stretching
2945	136	2940	143	2943	145	CH_3 symm stretching
3031	49	3024	49	3029	48	CH_2 symm stretching *xz* plane
3101	84	3095	104	3097	115	CH ring asymm stretching (1)
3107	44	3112	51	3121	50	CH ring asymm stretching (2)
3121	77	3135	47	3123	34	CH ring asymm stretching (3)
3138	36	3143	20	3144	18	CH ring symm stretching (1)
3146	156	3147	194	3148	205	CH ring symm stretching (2)

Number in parenthesis in assignment indicates the group reference of the vibration.

internal force constants and PED are not reported here, but can be downloaded as Supplementary material.

As in Part I, the surface was modeled by a single Ag atom at an initial distance of 3.0 Å in a position near perpendicular to the CN group for all the molecules under study. No constrains were used during the geometry optimization of the adsorbate–surface system.

3. Results and discussion

The quality of the present level of theory can be tested by comparison of our optimized geometrical parameters with current experimental values. In Fig. 1 are shown the optimized structures of *o*-methoxybenzonitrile (OMNB), *m*-methoxybenzonitrile (MMBN) and *p*-methoxybenzonitrile (PMBN). In general, the calculated geometrical parameters for these molecules (Table 1) are in good agreement with those obtained from NMR investigations of benzonitrile, BN [14] and those reported in Refs. [2,15,16].

The accuracy of the employed level of calculation can be also estimated from the good agreement of our calculated thermodynamic functions S^0 and C_p^0 with experimentally obtained data [4] for MMBN and PMBN at 298.15 K. These values are given in Table 2.

Fig. 2 shows the optimized structures of the molecule–Ag systems obtained in the SERS modelling. As expected, the Ag atoms are displaced from an almost right angle toward near linearity during the optimization. The calculated equilibrium position should be proportional to the SERS effect, and consequently produce intensity and/or frequency variation of some specific bands. While Table 3 gives calculated bond lengths for the OMBN–Ag, MMBN–Ag and PMBN–Ag systems, we present in Table 4 a comparison with those obtained in the Raman modelling. From this data it is observed that OMBN and MMBN have the same tilt in relation to the Ag atom, while the largest bent angle was calculated for PMBN. Furthermore, the shortest distance N–Ag corresponds to OMBN (shorter than the one in the BN–Ag system), while the longest N–Ag distance corresponds to PMBN. No significant changes are calculated in the ring-O and CN bond lengths in the presence of the Ag surface.

A selection of stretching (ν) force constants for the different isomers obtained at our theoretical level for Raman and SERS modelling is given in Table 5. The calculated values for the ring moiety are in agreement with those expected for aromatic systems, while

Table 7
Calculated SERS frequencies (cm^{-1}) and intensities ($Å^4$/amu) of the methoxybenzonitrile–Ag systems

OMBN–Ag		MMBN–Ag		PMBN–Ag		Assignment
Frequency	Intensity	Frequency	Intensity	Frequency	Intensity	
7	64	36	70	32	23	CH_3–BN–Ag bending *XZ*
76	207	67	147	61	101	CH_3–BN–Ag stretching
95	2	93	83	94	4	BN–O–CH_3 bending
137	28	149	16	134	23	CH_3–BN–Ag bending *YZ*
152	92	165	20	158	97	CH_3–BN–Ag bending *XY*
203	14	194	2	210	13	CH_3 torsion
238	21	242	3	240	1	BN–O–CH_3 in-plane bending
255	16	255	2	277	33	CH_3 rocking, BN out-of-plane bending
394	103	393	119	375	246	Ring symm in-plane deformation, CCN in-plane bending
403	17	400	186	412	2	CCN in-plane bending, C–O–CH_3 in-plane bending
443	449	458	411	472	22	Ring (CN) in-plane deformation
497	8	478	15	479	337	Ring asymm in-plane deformation, CCN out-of-plane bending
566	136	530	31	555	21	Ring (ortho) out-of-plane asymm deformation
573	9	586	33	561	12	Ring asymm out-of-plane deformation, CCN out-of-plane bending
591	36	623	3	639	12	CCN out-of-plane bending
709	406	691	7	661	19	Ring (ortho) in-plane symm deformation
749	4	696	148	734	10	CH asymm out-of-plane bending, ring out-of-plane deformation
769	4	802	1	791	239	CH symm in-plane bending
791	30	859	4	831	4	Ring breathing deformation, C–O stretching
872	1	902	1	853	12	CH asymm out-of-plane bending (1)
963	1	915	6	969	0	CH asymm out-of-plane bending (2)
980	365	975	450	981	34	Ring trigonal breathing, O–CH_3 stretching
1000	1	992	3	986	0	CH asymm out-of-plane bending (3)
1031	117	1012	21	997	28	Ring trigonal breathing (1)
1102	144	1086	0	1111	2	Ring trigonal breathing (2)
1115	8	1115	9	1116	8	CH_2 out-of-phase deformation
1152	19	1136	608	1157	10	CH_3 rocking
1174	20	1161	592	1175	385	CH ring in-plane bending
1184	76	1184	19	1195	237	Ring-CN stretching, CH_3 rocking
1241	128	1248	206	1240	71	Ring in-plane deformation, C–O stretching, CH_3 bending symm
1278	784	1294	6	1308	4	CH ring in-plane bending, CC ring stretching
1329	135	1344	26	1326	9	CC ring asymm stretching
1424	301	1422	6	1413	15	CC ring symm stretching, CH_3 symm bending
1444	63	1441	173	1440	22	CH_3 symm bed ring CC symm stretching
1466	11	1468	123	1469	24	CH_3 asymm bending *XY*
1470	20	1470	24	1471	20	CH_3 asymm bending *XY*, CC ring stretching
1481	266	1470	47	1493	407	CC ring symm stretching (1)
1573	219	1569	226	1555	8	CC ring symm stretching (2)
1591	6783	1603	3639	1607	1787	CC symm stretching, C–CN stretching
2187	25658	2186	25187	2178	14630	CN stretching
2947	234	2941	217	2945	270	CH_3 symm stretching
3034	55	3026	54	3032	52	CH_3 asymm stretching
3104	83	3097	126	3099	160	CH ring asymm stretching (1)
3109	19	3113	88	3121	63	CH ring asymm stretching (2)
3122	100	3136	27	3124	30	CH ring asymm stretching (3)
3138	60	3143	45	3145	43	CH ring symm stretching (1)
3147	327	3147	163	3148	227	CH ring symm stretching (2)

Number in parenthesis in assignment indicates the group reference of the vibration.

in the methoxy group the ring-O force constants are in the range provided by Durig and Daeyaert in an ab initio study of methoxydimethylphosphine [17]. Furthermore, C–OCH_3 and O–CH_3 force constants are comparable to those reported by Rao and Rao in a normal coordinate analysis of methoxyphenol [18]. Concerning the nitrile group, the DFT method slightly overestimates ν (C–CN) and ν (CN) values, partially due to the neglect of electron correlation and to basis set truncation. Values presented here for the nitrile group are comparable to those calculated in Ref. [19] in a HF calculation. In general, small differences between Raman and SERS force constants reflect the presence of the Ag atom. The small values calculated for the N–Ag force constants are consistent with the long distance between Ag and the different methoxybenzonitrile isomers.

In Tables 6 and 7 are presented band frequencies and their corresponding intensities obtained from the Raman and SERS spectra modelled for OMBN, MMBN and PMBN. Band assignments, also presented in these tables, have been obtained from the PED, and the analysis of animated normal modes. Raman frequencies and assignments of MMBN and PMBN can be compared with those calculated through out normal coordinate analysis [3] and experimental values [4,20,21]. The intensity calculation and the assignment of these bands are in agreement with the molecular orientation over the Ag atom shown in Fig. 2, as proposed by the SERS selection rules [6]. Comparing Raman and SERS normal modes assignment for the three isomers, it is noted that the most clear enhanced bands belong to the in-plane vibrations, and among them the biggest

Table 8
Correlation between experimental and calculated CN band: frequency and SERS-induced shift (cm^{-1}) for OMBN, MMBN and PMBN

	Experimental data [5]			This work		
	SERS	Raman	Δ	SERS	Raman	Δ
BN	2244	2230	14	2284*	2195*	89
OMBN	2234	2230	4	2268	2198	70
MMBN	2238	2231	7	2278	2196	82
PMBN	2230	2228	2	2225	2189	36

*Part I.

Table 9
Correlation between experimental and calculated 8a band: frequency and SERS-Raman intensity ratio for OMBN, MMBN and PMBN

	Experimental data [5]		This work	
	Frequency (cm^{-1})	I_{SERS}/I_{Raman}	Frequency (cm^{-1})	I_{SERS}/I_{Raman}
OMBN	1574	9.7	1591	85
MMBN	1603	3.7	1603	58
PMBN	1602	1.3	1607	10

Table 10
Frontier orbital energies (a.u.) of the investigated systems

	OMBN	OMBN–Ag	MMBN	MMBN–Ag	PMBN	PMBN–Ag
LUMO	−0.057	−0.077	−0.059	−0.081	−0.051	−0.078
HOMO	−0.246	−0.255	−0.248	−0.254	−0.246	−0.255
Δ	0.189	0.178	0.189	0.173	0.195	0.177

LUMO OMBN–Ag–FL = 0.125 a.u. (365 nm).
FL–HOMO OMBN–Ag = 0.053 a.u. (860 nm).
LUMO MMBN–Ag–FL = 0.121 a.u. (377 nm).
FL–HOMO MMBN–Ag = 0.052 a.u. (876 nm).
LUMO PMBN–Ag–FL = 0.124 a.u. (367 nm).
FL–HOMO PMBN–Ag = 0.053 a.u. (860 nm).

intensity enhancements are observed for the CN stretching in the order OMBN > MMBN > PMBN. The difference between the SERS and Raman CN frequency (cm^{-1}) calculated in the present work for the distinct isomers is correlated to the experimental data reported in Ref. [5] (Table 8).

This sequence is inversely correlated to the N–Ag distance, the more tilted PMBN–Ag system with the longest bond is the least influenced by the attachment of a silver atom. The calculated intensity enhancements can be compared with the most relevant intensity enhancement given in Ref. [5]. Therein, an order of enhancement for the three MBNs is found, for instance the 8a band assigned to a CC in-plane stretching, where the least enhanced band corresponds to the PMBN isomer (Table 9).

In analogy to the results for BN in Part I, it is possible from the data above to infer that a charge transfer (CT) mechanism should be dominant in the SERS spectra of the three isomers. In this part of the work we have therefore investigated the Frontier orbitals of the adsorbates. The results given in Table 10 show that the HOMO–LUMO gap for OMBN (241 nm), MMBN (241 nm), and PMBN (234 nm) reproduce quite well the absorption maxima λ_{max} reported by Tsuzuki and Asabe [22] for the L_c-band of the electronic spectra of these molecules at 232, 230 and 248 nm, respectively. Table 10 also shows that the presence of the Ag atom leads to a reduction of the HOMO–LUMO gap. The effect is similar for all three isomers and the energy differences resemble those determined for the BN–Ag system. Taking into account that the difference in energy between the Ag Fermi level (FL, −0.202 a.u.) [23] and the Frontier orbitals, as well as the frequency of the incident light (514 nm) [5] we can classify the chemical enhancement [24,25] as a ligand to metal charge transfer process for the methoxybenzonitriles, in analogy to BN. A metal to ligand CT process can be ruled out as the required energy cannot come from the laser excitation.

4. Summary and conclusions

The model and the level of theory employed in Part I prove to be useful in the modelling of the Raman and SERS spectra of the distinct methoxy derivatives of benzonitrile. The optimized structures of the methoxybenzonitrile–Ag system confirm the importance of the nitrogen lone pair electrons in the SERS process for these molecules. Examination of frequencies which experience an important change in intensity after passing from Raman to SERS spectrum reveals that most of them are assigned to in-plane normal modes, in agreement with the surface selection rules for perpendicular orientation of molecules.

In Ref. [2] are reported experimental correlations similar to those presented above, however, in that work it is postulated that the benzene ring in MMBN is orientated perpendicular to the silver surface, whereas the benzene ring of both the *ortho*- and *para*-derivatives assume tilted stances with respect to the silver surface. This assumption is based on the strong resonance donor power of methoxy group in the *para*-isomer, although the authors recognize that to justify this argument, more extensive SERS studies on various benzonitriles derivatives should be performed. In the meanwhile, the present theoretical study is not only useful to point towards a different non-perpendicular orientation for MMBN but also to give insight on the characteristics of the SERS spectra for the three-methoxybenzonitrile isomers.

From our results it is possible to interpret the effect of a metallic surface on the distinct isomers. In this sense, correlations obtained from Raman and SERS data among optimized geometry parameters, force constants, changes in frequencies and intensities show that the proximity of the CN to the methoxy group has influence on the orientation of these molecules on the Ag atom. Accordingly, the SERS effect in the three isomers should be in the sequence OMBN–MMBN > PMBN. Theoretical concepts on SERS developed in literature are also well represented: the calculated HOMO–LUMO gap for the three isomers reproduce quite well the electronic spectra of these molecules, while for the molecule–Ag systems the HOMO–LUMO energies allow us derive a main contribution of ligand to metal CT mechanism.

Acknowledgements

The authors acknowledge projects Fondecyt 1040640 and 107078. GDF also acknowledges DGI Universidad de Playa Ancha. RK is grateful for a generous allocation of computing time at the CSC, Uni Oldenburg.

Appendix A. Supplementary data

Supplementary data associated with this article can be found, in the online version, at doi:10.1016/j.saa.2008.03.007.

References

[1] G. Diaz Fleming, I. Golsio, A. Aracena, F. Celis, L. Vera, R. Koch, M. Campos-Vallette, Spectrochim. Acta Part A 71 (2008) 14049.
[2] A.P. Kumar, G.R. Rao, Spectrochim. Acta 53A (1997) 2023.
[3] A.P. Kumar, G.R. Rao, Spectrochim. Acta 53A (1997) 2041.
[4] R.K. Goel, M.L. Agarwal, Spectrochim. Acta 38A (1982) 583.
[5] D.W. Boo, M.S. Kim, K. Kim, Bull. Korean Chem. Soc. 9 (1988) 311.
[6] J.A. Creighton, in: R.J.H. Clark, R.E. Hester (Eds.), Spectroscopy of Surfaces—Advances in Spectroscopy, vol. 16, Wiley, New York, 1988, p. 37 (chapter 2).
[7] M.J. Frisch, G.W. Trucks, H.B. Schlegel, G.E. Scuseria, M.A. Robb, J.R. Cheeseman, J.A. Montgomery Jr., T. Vreven, K.N. Kudin, J.C. Burant, J.M. Millam, S.S. Iyengar, J. Tomasi, V. Barone, B. Mennucci, M. Cossi, G. Scalmani, N. Rega, G.A. Petersson, H. Nakatsuji, M. Hada, M. Ehara, K. Toyota, R. Fukuda, J. Hasegawa, M. Ishida, T. Nakajima, Y. Honda, O. Kitao, H. Nakai, M. Klene, X. Li, J.E. Knox, H.P. Hratchian, J.B. Cross, C. Adamo, J. Jaramillo, R. Gomperts, R.E. Stratmann, O. Yazyev, A.J. Austin, R. Cammi, C. Pomelli, J.W. Ochterski, P.Y. Ayala, K. Morokuma, G.A. Voth, P. Salvador, J.J. Dannenberg, V.G. Zakrzewski, S. Dapprich, A.D. Daniels, M.C. Strain, O. Farkas, D.K. Malick, A.D. Rabuck, K. Raghavachari, J.B. Foresman, J.V. Ortiz, Q. Cui, A.G. Baboul, S. Clifford, J. Cioslowski, B.B. Stefanov, G. Liu, A. Liashenko, P. Piskorz, I. Komaromi, R.L. Martin, D.J. Fox, T. Keith, M.A. Al-Laham, C.Y. Peng, A. Nanayakkara, M. Challacombe, P.M.W. Gill, B. Johnson, W. Chen, M.W. Wong, C. Gonzalez, J.A. Pople, Gaussian 03, Revision B. 05, Gaussian Inc., Pittsburgh, PA, 2003.
[8] A.D. Becke, J. Chem. Phys. 98 (1993) 1372.
[9] C. Lee, W. Yang, R.G. Parr, Phys. Rev. B 37 (1988) 785.
[10] T.H. Dunning, P.J. Hay, in: H.F. Schaefer (Ed.), Methods of Electronic Structure Theory, vol. 2, Plenum Press, New York, 1977.

[11] P.J. Hay, W.R. Wadt, J. Chem. Phys. 82 (1985) 299.
[12] A.P. Scott, L. Radom, J. Phys. Chem. 100 (1996) 16502.
[13] W.B. Collier, QCPE Bull. 13 (1993) 19.
[14] P. Diehl, J. Amerin, C.A. Veracini, Org. Magn. Reson. 20 (1982) 276.
[15] P. Kumaradhas, N. Kalyanam, K.A. Nirmala, Cryst. Res. Technol. 36 (2001) 1435.
[16] A. Philippou, F. Salehirad, D.-P. Luigi, M.W. Anderson, J. Chem. Soc., Faraday Trans. 94 (1998) 2851.
[17] J.R. Durig, F.F.D. Daeyaert, J. Mol. Struct. (Theochem.) 261 (1992) 133.
[18] P.V.R. Rao, G.R. Rao, Spectrochim. Acta Part A 58 (2002) 3039.
[19] A.G. Csaszar, G. Fogarasi, Spectrochim. Acta 45A (1989) 845.
[20] G. Varsany, Assignment for Vibrational Spectra of Seven Hundred Benzene Derivatives, vol. I, Adam Hilger, London, 1974, and references cited therein.
[21] C.L. Chaterjee, P.P. Garg, R.M.P. Jaiswal, Spectrochim. Acta Part A 34 (1978) 9432.
[22] Y. Tsuzuki, Y. Asabe, J. Chem. Eng. Data 16 (1971) 108.
[23] N.W. Aschcroft, D.N. Mermin, Solid State Physics, W.B. Saunders Co., Philadelphia, London, Toronto, 1976.
[24] A. Campion, P. Kambhampati, Chem. Soc. Rev. 27 (1998) 241.
[25] A.M. Michael, J. Jiang, L. Brus, J. Phys. Chem. B 104 (2000) 11965.